Journal of Applied Sciences

ISSN 1812-5654

science alert

ANSInet
an open access publisher
http://ansinet.com

Journal of Applied Sciences 15 (4): 633-643, 2015
ISSN 1812-5654

ansinet
Asian Network for Scientific Information

RESEARCH ARTICLE OPEN ACCESS

DOI: 10.3923/jas.2015.633.643

Closed Loop Controlled Soft Switching Type DC/DC Converter with High Efficiency under Variable Load Conditions

[1]Deepak Kumar Nayak, [1]S. Sheik Aalam, [1]R. Murugan and [2]S. Rama Reddy
[1]Department of ECE, Aalim Muhammed Salegh College of Engineering, Muthapudupet, Avadi, IAF, Chennai, 600055, India
[2]Department of EEE, Jerusalem College of Engineering,
Centre for Collaborative Research with Anna University, Pallikaranai, Chennai, 600100, India

ARTICLE INFO
Article History:
Received: December 01, 2014
Accepted: January 21, 2015

Corresponding Author:
Deepak Kumar Nayak,
Department of ECE,
Aalim Muhammed Salegh College of Engineering, Muthapudupet, Avadi,
IAF, Chennai, 600055, India

ABSTRACT
A full bridge DC/DC converter with an auxiliary circuit and a voltage doubler type rectifier is proposed in this study. Due to the auxiliary circuit, the proposed circuit achieves Zero Voltage Switching (ZVS) for main switches and Zero Current Switching (ZCS) for auxiliary switches to provide reduced switching stress and high efficiency. Since there is no output inductor, the voltage across the rectifier diodes can be clamped to the output voltage level and it features a simple structure. The operation of the new converter is explained, analyzed and implemented in MATLAB with 20 kHz switching frequency and 15 W output power. Open loop and closed loop models are presented for input step change and output load regulation.

Key words: DC/DC converter, zero voltage switching, zero current switching, soft-switching, full bridge converter

INTRODUCTION

Full bridge converters have been widely used in high power applications (Sabate *et al*., 1990; Lee *et al*., 2008; Nayak and Reddy, 2011; Kathirvelu and Balasubramanian, 2014). These converters provide zero voltage switching of primary switches with a relatively small circulating energy. However, the disadvantage is that to achieve ZVS for the lagging leg switches under light load conditions require a large inductance in series with the primary winding of the transformer. The increased inductance produces an increased loss of duty cycle on the secondary side and more voltage ringing across the secondary side rectifiers.

Many methods have been proposed to achieve ZVS for the lagging leg switches under extended load conditions. Extra passive components are used to achieve full range ZVS by Jain *et al*. (2002) and Wu *et al*. (2006). However, there is significant amount of conduction loss which reduces the efficiency of the converter.

To achieve full range ZVS extra active components are used on the primary side (Bakan *et al*., 2013; Cho *et al*., 2011). The advantages of these topologies are the conduction loss is decreased and the secondary side voltage spikes are reduced but it uses two additional main switches in the primary side which increases the cost and due to circuit complexity it is difficult to implement.

To achieve full range ZVS, extra active components are used on the secondary side (Cacciato and Consoli, 2011) but it does not address the free wheeling period conduction loss and the secondary side voltage ringing. By adding an active snubber described by Sabate *et al*. (1991) and Mishima and Nakaoka (2011), the secondary side voltage ringing can be suppressed but it adds to cost and it is difficult to implement.

A current driven rectifier is introduced by Pahlevaninezhad *et al*. (2012) which provides zero current switching for output rectifiers with the help of two parallel passive circuits. As proposed by Chen *et al*. (2012), parasitic mechanism and suppression counter measure of voltage oscillation for the full bridge converter is analyzed in detail but the proposed LC auxiliary circuit only extends the ZVS range of the lagging leg switches while ZVS range of the leading leg switches cannot be attained at light load conditions. In

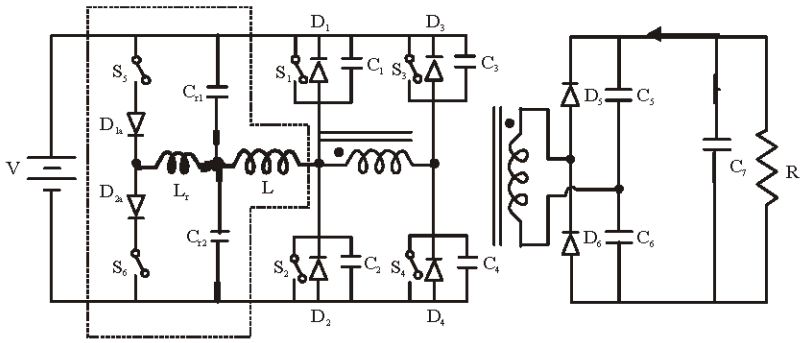

Fig. 1: Proposed full bridge DC/DC converter

Yadav and Narasamma (2014), a soft switching full bridge converter with an auxiliary circuit is proposed which achieves soft switching for both main and auxiliary switches for providing high efficiency.

In this study, a new soft switching DC/DC converter is proposed with a full ZVS range by combining the LCCL auxiliary circuit and voltage doubler type rectifier. The proposed LCCL network is connected in parallel to the lagging leg and voltage doubler type rectifier is connected at the secondary side of the transformer as shown in Fig. 1. The operation of the proposed converter is explained in detail. The simulation model of the proposed converter is designed in MATLAB simulink and it was implemented a 15 W/12 V output.

MATERIALS AND METHODS

Converter operation and analysis: Figure 1 shows the proposed full bridge DC/DC converter with an auxiliary circuit indicated in dotted lines. For simplified reason leakage inductance and magnetic inductance are not shown in Fig. 1. The main switches of full bridge are S_1 to S_4. The auxiliary circuit proposed here contains two active switches S_5 and S_6, two diodes D_{1a} and D_{2a}, resonant capacitor C_{r1} and C_{r2}, resonant inductor L_r and coupling winding L. Figure 2 shows the driving signals for all main switches, auxiliary switches and the principal waveforms. Gating pulse for the auxiliary switch S_6 is given, when the main switch S_1 is turned off and before S_2 is on. Similarly gating pulse for the auxiliary switch S_5 is given, when the main switch S_2 is turned off and before S_1 is turned on.

The proposed converter has 10 operation modes during a switching cycle. Prior to mode1, body diode D_1 and S_4 are conducting. Body diode D_1 provides ZVS turn on for switch S_1 when it is on at mode 1.

Mode 1 [t_0 t_1]: As shown in Fig. 3a, at $t = t_0$, S_1 and S_4 are on and rectifier diode D_5 is on. A positive voltage appears across the transformer secondary dotted end and positive power transfer happens in this interval.

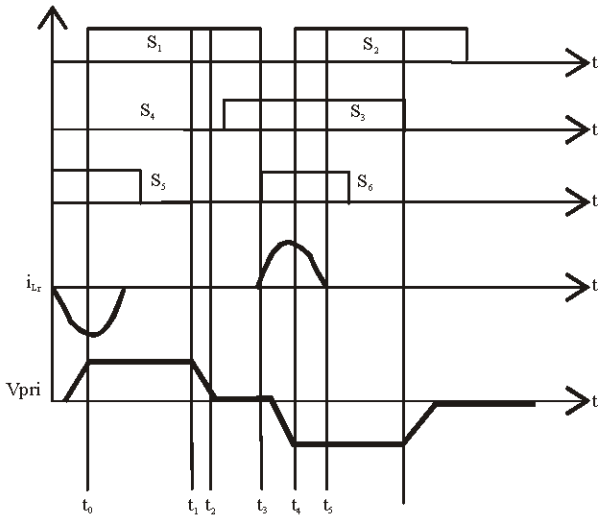

Fig. 2: Waveforms of the proposed full bridge DC/DC converter

Let $C_1 = C_2 = C_3 = C_4 = C$ and $C_{r1} = C_{r2} = C_r$

L_m = Magnetizing inductance of the transformer
L_P = Leakage inductance of the transformer
i_m = Magnetizing current
I_0 = Output current
n = Turns ratio of the transformer
i_1 = Reflected load current
V_{pri} = Voltage across the primary of the transformer
I_{pri} = Current across the secondary of the transformer

Voltage and current across the primary of the transformer is given as:

$$V_{Pri}(t-t_0)=\frac{L_m di_m(t-t_0)}{dt}=V \quad (1)$$

$$I_{Pri}=\frac{1}{n}\left[\frac{V}{n}-V_0(t_0)\right]\frac{1}{Z_0}\sin w_r(t-t_0)+I_m(t-t_0) \quad (2)$$

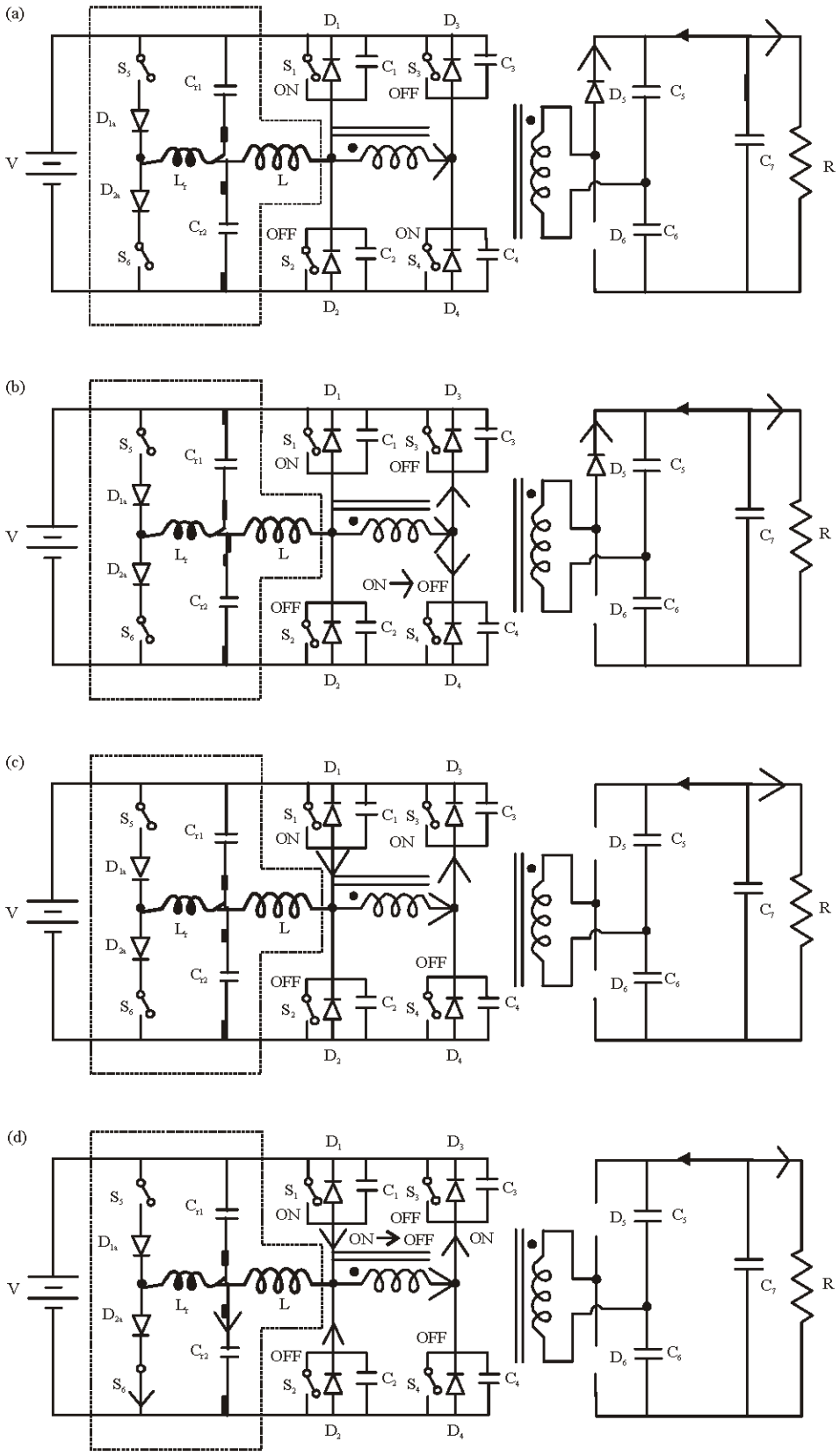

Fig. 3(a-e): Continue

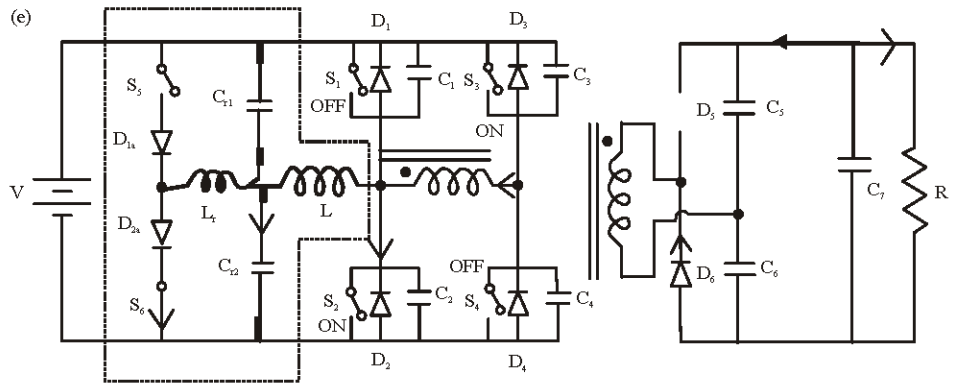

Fig. 3(a-e): Operating circuits during the first half cycle: (a) Mode 1, (b) Mode 2, (c) Mode 3, (d) Mode 4 and (e) Mode 5

Where:

$$w_r = \frac{n}{\sqrt{L_P C_r}},\ Z_0 = \frac{1}{n}\sqrt{\frac{L_P}{C_r}} \text{ and } C_r = \frac{C_5}{C_6}$$

At the end of this mode at $t = t_1$:

$$V_{C_2}(t_2) = V_{C_4}(t_2) = V \text{ and } V_{C_1}(t_2) = V_{C_3}(t_2) = 0$$

Mode 2 [t_1 t_2]: As shown in Fig. 3b, S_4 is off. The primary current which was flowing through S_4 charges the output capacitance of S_4 and discharges the output capacitance of S_3. The voltage across the transformer primary side V_{Pri} is decreased to 0 V. Rectifier diodes D_6 continue to conduct. At the end of this interval, switch S_3 can be turned on at ZVS because body diode D_3 is forward biased. At the end of this mode at $t = t_2$:

$$V_{C_2}(t_2) = V_{C_4}(t_2) = V \text{ and } V_{C_1}(t_2) = V_{C_3}(t_2) = 0$$

Mode 3 [t_2 t_3]: As shown in Fig. 3c, the ZVS operation of the leading leg takes place by utilizing the energy stored in the leakage inductor and magnetizing inductor:

$$V_{Pri}(t - t_2) = L_m \frac{di_m(t - t_2)}{dt} \quad (3)$$

At the end of this mode at $t = t_3$:

$$V_{C_2}(t_3) = V_{C_4}(t_3) = V \text{ and } V_{C_1}(t_3) = V_{C_3}(t_3) = 0$$

Mode 4 [t_3 t_4]: As shown in Fig. 3d, S_1 is off and the auxiliary switch S_6 is on. Resonant current flows through the resonant inductor L_r and resonant capacitor C_{r2}. The resonant current i_{L_r} and resonant capacitor voltage V_{C_r} are given by:

$$i_{L_r}(t - t_4) = nI_0 + V\sqrt{\frac{C_r}{L_r}}\sin\left(w(t - t_3)\right) \quad (4)$$

$$V_{C_r}(t - t_4) = V\cos\left(w(t - t_3)\right) \quad (5)$$

At the end of this mode, body diode of S_2, D_2 starts conducting to ensure ZVS turn on for S_2. The resonant capacitor voltage at the end of this mode is given as:

$$V_{C_r} = \left(\frac{-V}{K_T}\right) \quad (6)$$

where, K_T is turns ratio between primary winding of transformer and coupled winding. At the end of this mode, output rectifier diode D_6 starts conducting full load current. At the end of this mode at $t = t_4$:

$$V_{C_1}(t_4) = V_{C_4}(t_4) = V \text{ and } V_{C_2}(t_4) = V_{C_3}(t_4) = 0$$

Mode 5 [t_4 t_5]: As shown in Fig. 3e, resonant capacitor voltage ($-V/K_T$), at the end of mode 4, resets the resonant current linearly to zero. So, the switch S_6 is turned off at ZCS. Output rectifier D_6 conducts in the same direction. At the end of this interval at $t = t_5$:

$$V_{C_1}(t_6) = V_{C_4}(t_6) = V \text{ and } V_{C_2}(t_6) = V_{C_3}(t_6) = 0$$

Mode 6-10 is same as mode 0-5.

The ZVS operation of the leading leg takes place by utilizing the energy stored in the leakage inductor and magnetizing inductor. The ZVS operation of the lagging leg takes place by utilizing the energy stored in the magnetizing inductor. From this analysis, we are observing soft switching for both main and auxiliary switches without increasing the main device voltage/current rating.

RESULTS AND DISCUSSION

Simulation results: The proposed converter is simulated using MATLAB simulink. The specifications and the component values of the converter are shown in Table 1.

Gating signals for lagging leg switches (S_1 and S_2) and auxiliary switches (S_5 and S_6) are shown in Fig. 4a. It is observed that the conduction time of the main switches are longer than the auxiliary switches. The auxiliary switch S_6 is on when lagging leg switch S_1 is off and the auxiliary switch

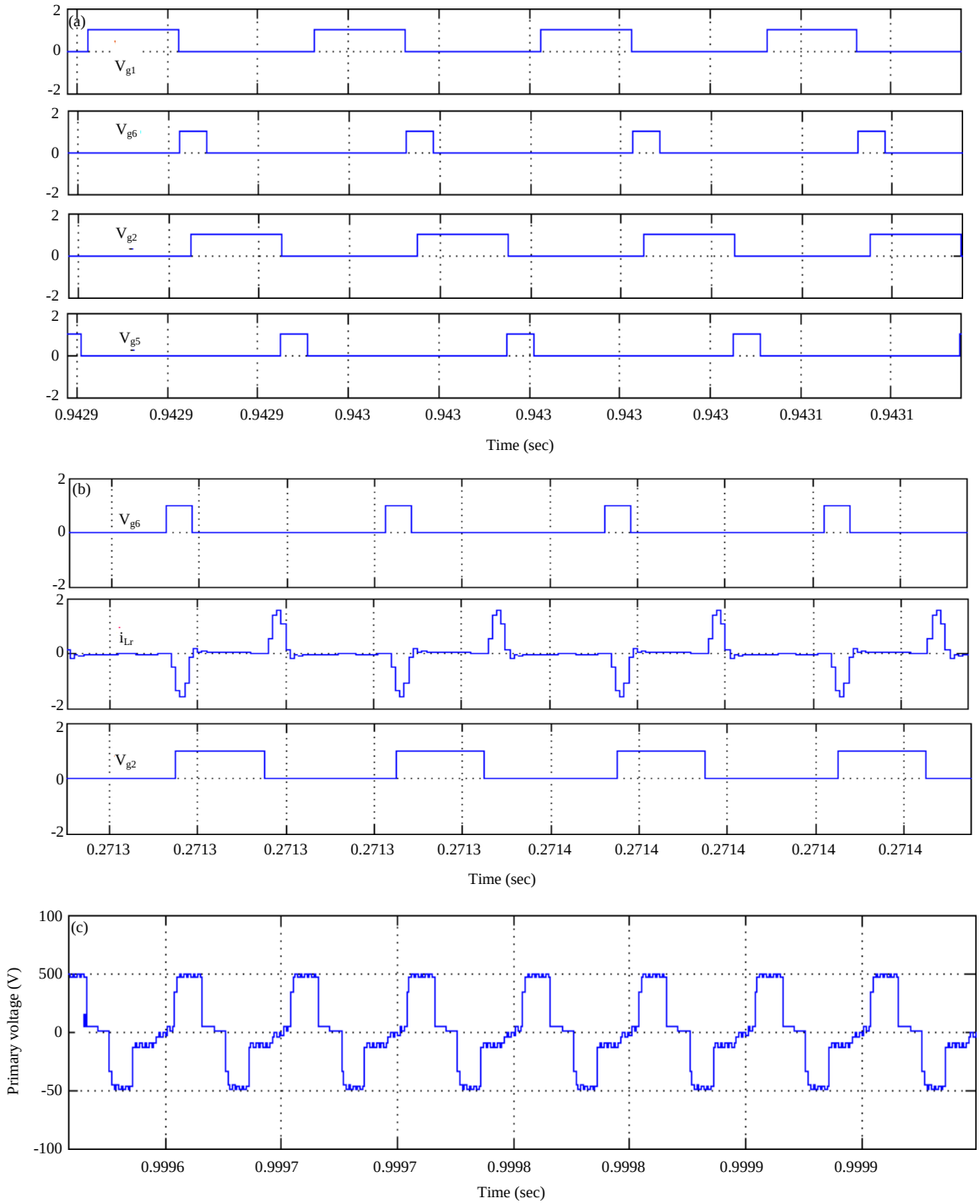

Fig. 4(a-f): Continue

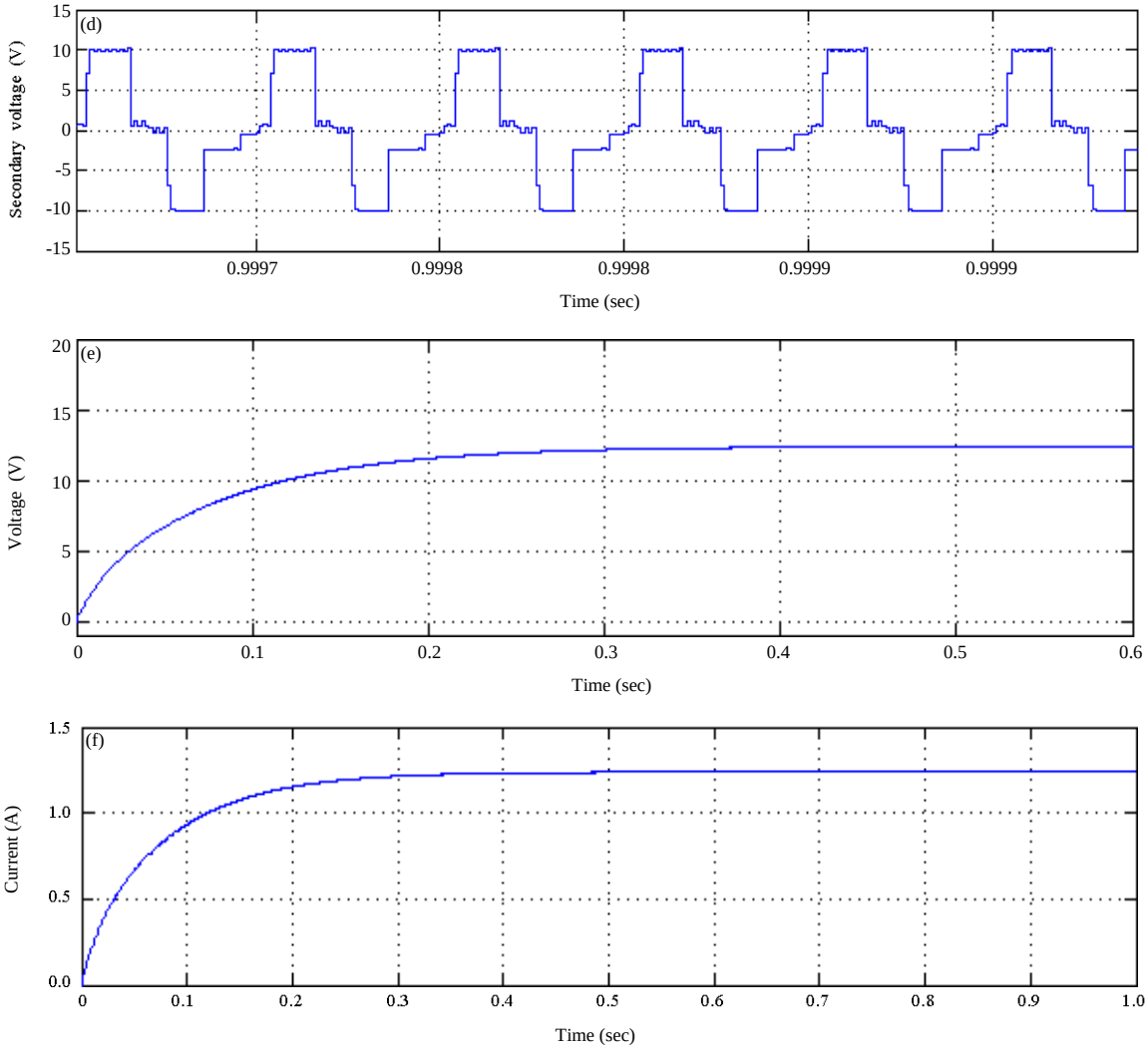

Fig. 4(a-f): Simulation waveforms, (a) Driving pulses of S_1, S_5, S_2 and S_6, (b) Driving pulses of S_6, resonant inductor current i_{L_r}, Driving pulses of S_2, (c) Primary voltage of the transformer, (d) Secondary voltage of the transformer, (e) DC output voltage and (f) DC output current

Table 1: Converter specifications and component values

Specification	Component values
Input voltage: V = 48 V	Auxiliary inductance: L_r = 0.1 mH
Output voltage: V_0 = 12 V	Auxiliary capacitance: C_r = 0.015 μF
Switching frequency: f = 20 kHz	Coupling inductance: L = 90 H
Power: P = 15 W	Rectifier capacitance: $C_5 = C_6$ = 5 μF
	Filter capacitance: C_7 = 25 mF

Table 2: Performance of the proposed converter from simulation

Load (%)	Output voltage (V)	Output current (A)	Output power (W)	Input power (W)	Efficiency (%)
54	12.47	0.71	8.85	9.60	92.15
66	12.44	0.87	10.82	11.65	92.85
70	12.42	0.92	11.43	12.27	93.17
85	12.39	1.11	13.75	14.70	93.51
95	12.38	1.24	15.35	16.36	93.80
100	12.36	1.31	16.19	17.16	94.34

S_5 is on when lagging leg switch S_2 is off. The gating signals for S_6, resonant inductor current i_{L_r}, gating signal of S_2 and drain to source voltage of S_2 are shown in Fig. 4b. It is seen that the resonant inductor current is zero before gating signal for S_6 becomes zero which ensures Zero Current Switching (ZCS) for S_6 (auxiliary switch). The primary voltage and secondary voltage of the transformer is shown in Fig. 4c and 4d, respectively. DC output voltage is 12 V as shown in Fig. 4e and DC output current is 1.2 A as shown in Fig. 4f. The performance of the proposed converter from simulation measurement is given in Table 2. The efficiency of the proposed converter and the conventional converter as a function of load current is shown in Fig. 5. From Fig. 5, it can be seen that the efficiency of the proposed converter is higher than that of the conventional converter. The

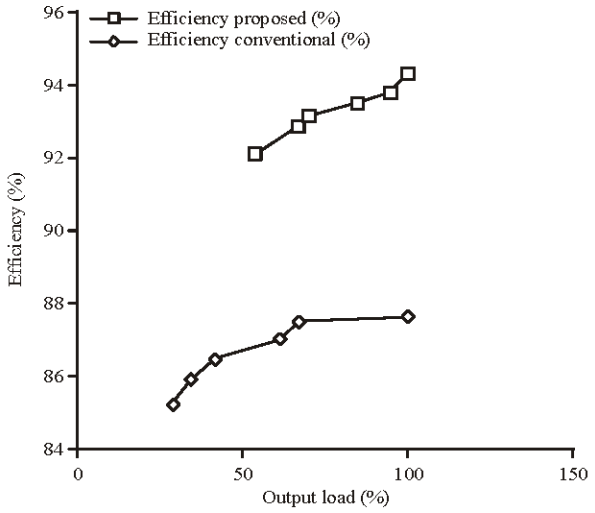

Fig. 5: Efficiency versus load current from simulation

efficiency decreases at light load but over a wide load current range, the efficiency curve remains flat.

The efficiency of the proposed converter is 6% higher than that of the converter reported by Nayak and Reddy (2011). The use of the transformer and absent of the output inductor in the proposed circuit reduces the size of the converter.

Comparison of open loop system with closed loop system for input step change: Figure 6 shows the block diagram of the closed loop system. Figure 7 shows the open loop based simulink model of the proposed circuit with an input disturbance at 0.75 sec. We observe from Fig. 8 that, the output voltage changes with the change in input voltage. Figure 9 shows the closed loop simulink model of the proposed circuit with an input disturbance at 0.75 sec. The closed loop model uses a comparator where the instantaneous output voltage is compared with the set voltage of 12 V.

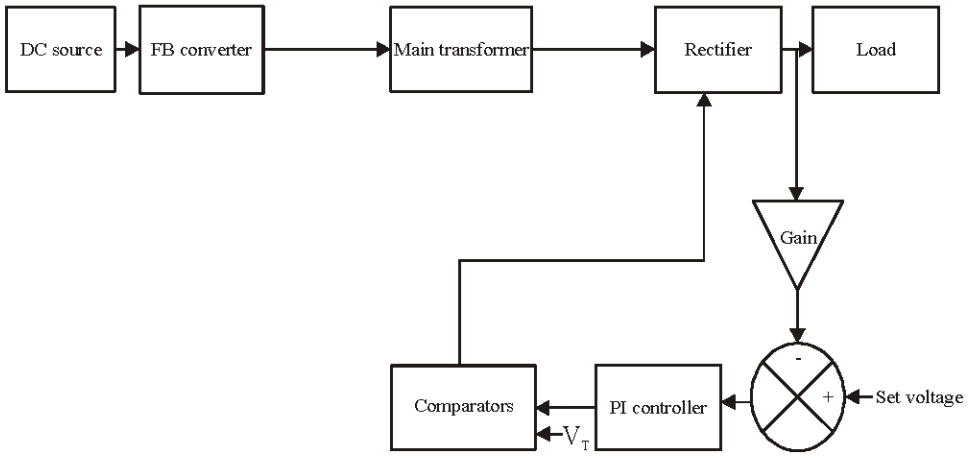

Fig. 6: Block diagram of closed loop system

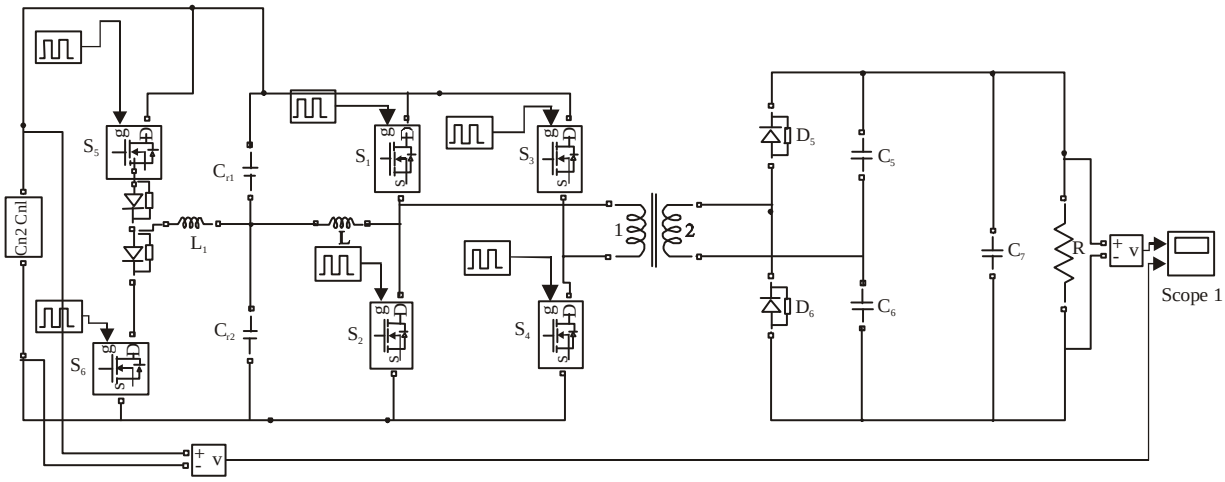

Fig. 7: Open loop system with input step change

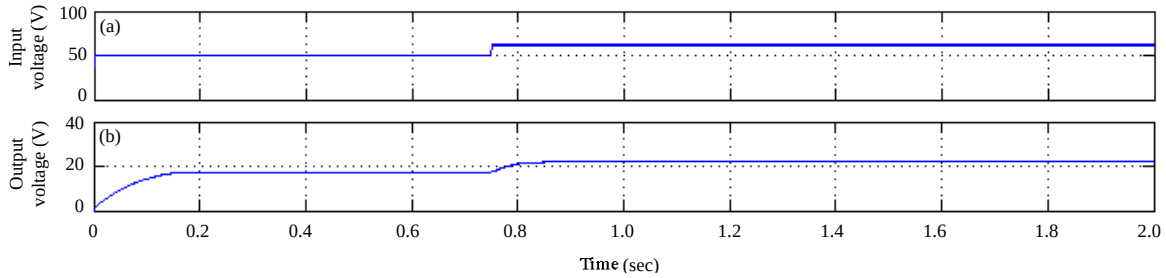

Fig. 8(a-b): (a) Input and (b) Output voltage with input step change

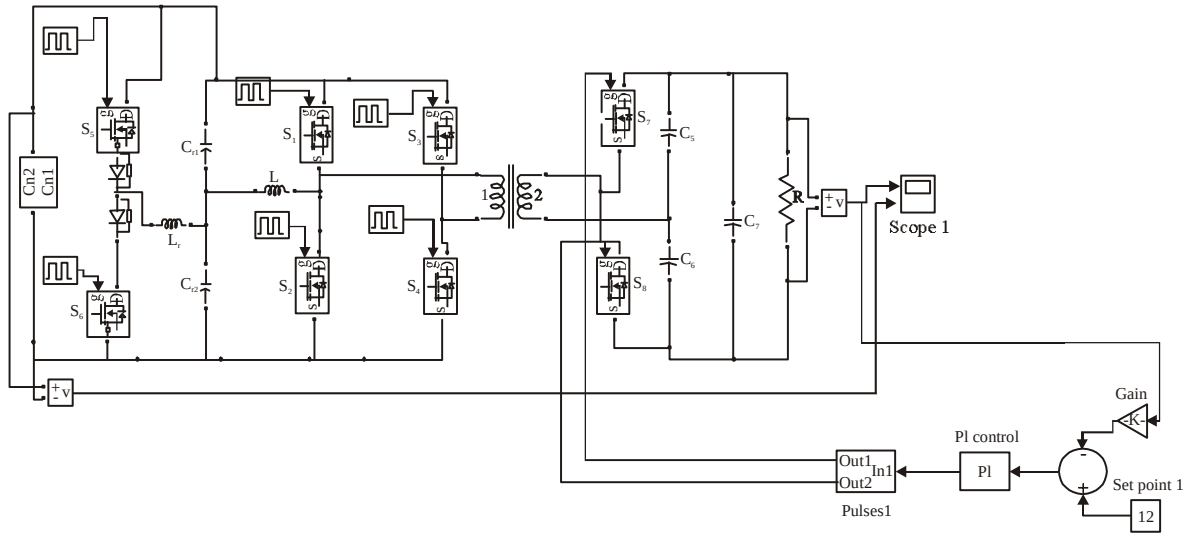

Fig. 9: Closed loop system with input step change

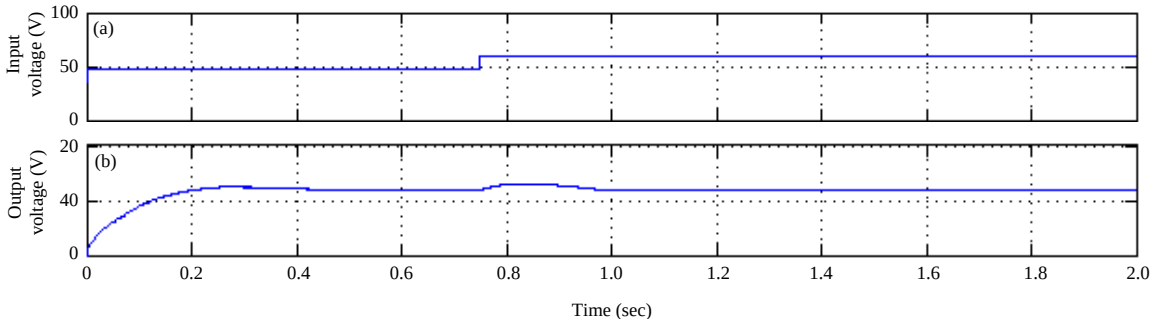

Fig. 10(a-b): (a) Input and (b) Output voltage with input step change (closed loop)

The output voltage of the comparator is applied to the PI controller which controls the output voltage of the closed loop system. We observe from Fig. 10 that, the output voltage increases and due to the close loop action, reduces to 12 V. So, the steady state error is reduced by using the closed loop system.

Comparison of open loop system with closed loop system for output load regulation: Figure 11 shows the open loop based simulink model of the proposed converter without output load regulation. The load resistance of 10 is connected through a breaker and additional resistance of 10 is connected through the breaker. Initially the breaker is opened and it is closed at 0.4 S. Due to the change in the load, the DC output voltage changes at 0.4 S but DC input voltage is constant 48 V as shown in Fig. 12. Figure 13 shows the closed loop based simulink model of the proposed converter with output load regulation. The subtractor in the closed loop has two

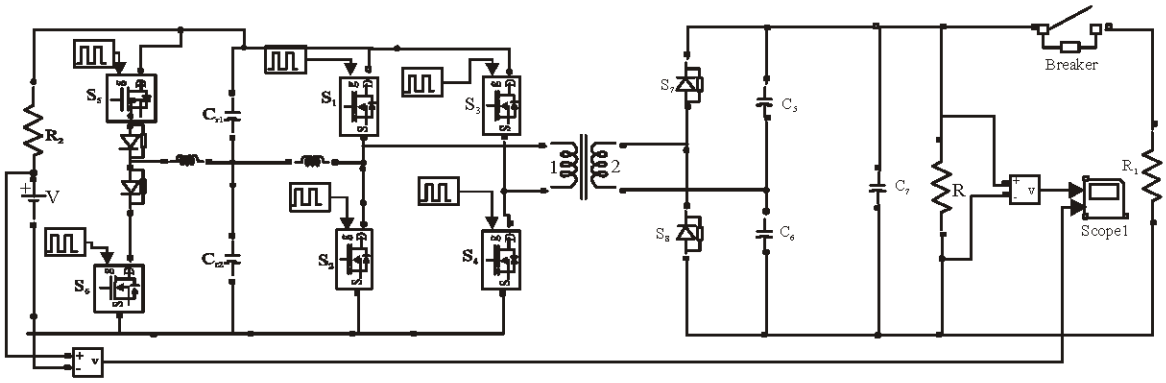

Fig. 11: Open loop system without output load regulation

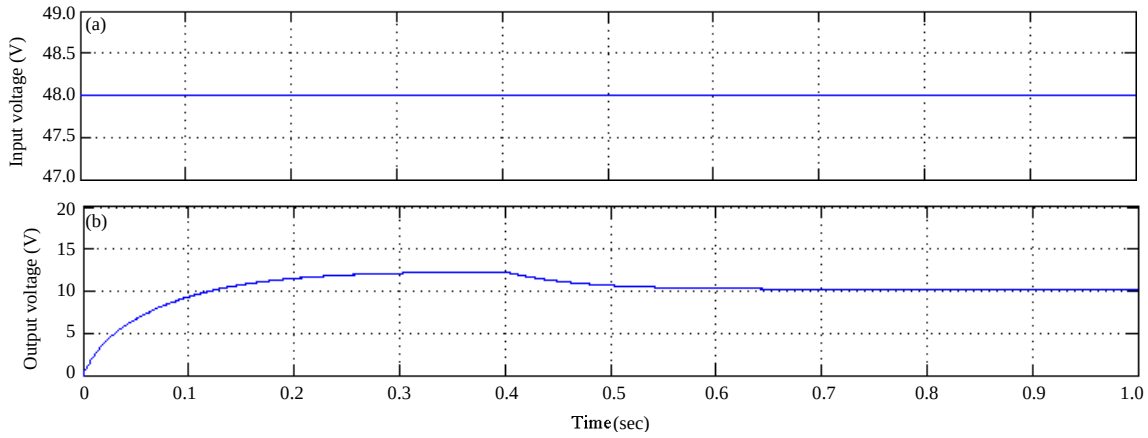

Fig. 12(a-b): DC (a) Input and (b) Output voltage without load regulation

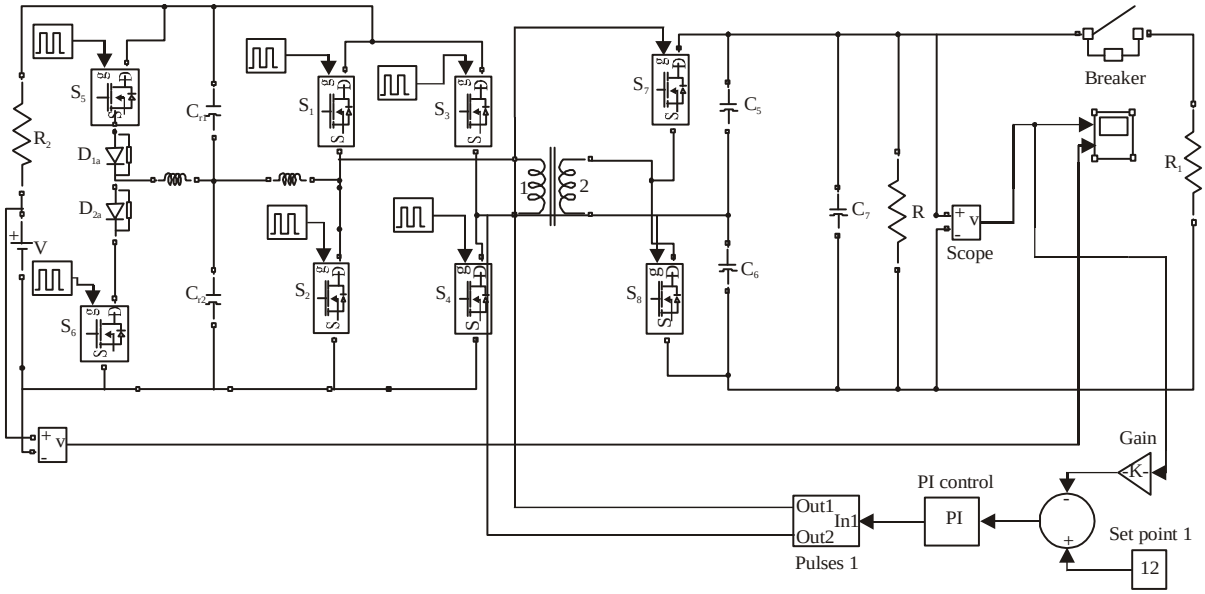

Fig. 13: Closed loop system with output load regulation

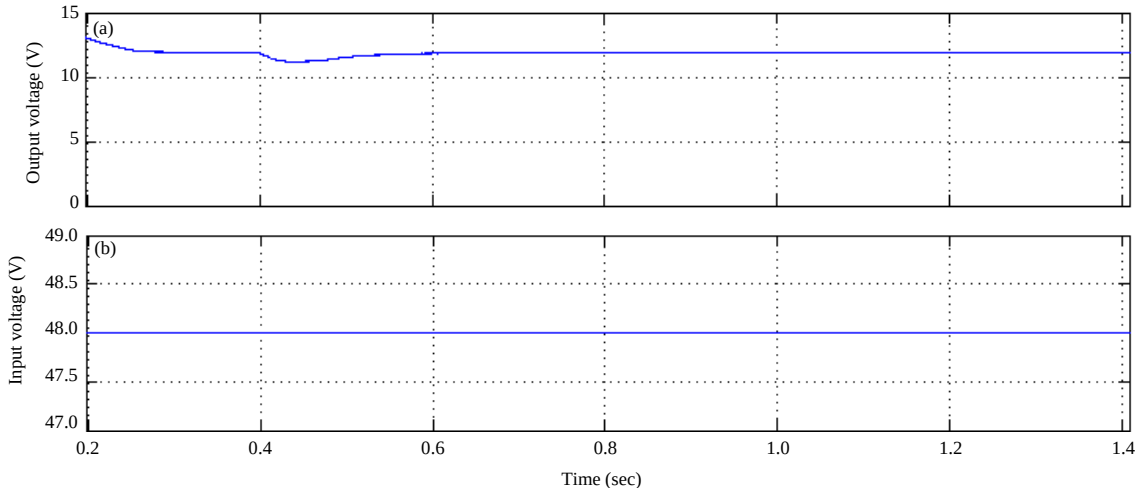

Fig. 14(a-b): DC Output voltage with Output load regulation

inputs. One input is the instantaneous output voltage and another input is the reference or set voltage of 12 V. The output of the subtractor is given to the PI controller. The PI controller output is given to the two comparators and the two comparator outputs are given as control signals to the gate pulses for switches S_7 and S_8. Initially the breaker is opened and it is closed at 0.5 S. We observe that, the DC output voltage reduces at 0.5 S when the breaker is closed and due to the closed loop control, final steady state output voltage reaches to a value of 12 V as shown in Fig. 14.

CONCLUSION

A new soft switched full bridge DC/DC converter has been proposed in this study. The proposed converter employs an LCCL network as auxiliary circuit with a voltage doubler type rectifier without an output inductor. The operation and performance of the proposed circuit is analyzed in detail and a prototype is developed in MATLAB simulink. The ZVS operation of the leading leg takes place by utilizing the energy stored in the leakage inductor and magnetizing inductor. The ZVS operation of the lagging leg takes place by utilizing the energy stored in the magnetizing inductor. Conversion of 48-12 V is done by using the proposed converter and the results are compared with a conventional converter. It has been found that the proposed converter has higher efficiency in comparison to conventional converter. The other advantage is that there is no inductor in the output of the rectifier. The proposed converter is expected to be suitable for medium to high power applications because of high efficiency.

REFERENCES

Bakan, A.F., N. Altintas and I. Aksoy, 2013. An improved PSFB PWM DC-DC converter for high-power and frequency applications. IEEE Trans. Power Electron., 28: 64-74.

Cacciato, M. and A. Consoli, 2011. New regenerative active snubber c ircuit for ZVS phase shift full bridge converter. Proceedings of the 26th Annual IEEE Applied Power Electronics Conference and Exposition, March 6-10, 2011, Fort Worth, TX., USA., pp: 1507-1511.

Chen, Z., L. Shi, F. Ji and S. Liu, 2012. Mechanism and suppression countermeasure of voltage oscillation for full bridge converter. IET Trans. Power Electron., 5: 1535-1543.

Cho, I.H., K.M. Cho, J.W. Kim and G.W. Moon, 2011. A new phase-shifted full-bridge converter with maximum duty operation for server power system. IEEE Trans. Power Electron., 26: 3491-3500.

Jain, P.K., W. Kang, H. Soin and Y. Xi, 2002. Analysis and design considerations of a load and line independent zero voltage switching full bridge DC/DC converter topology. IEEE Trans. Power Electron., 17: 649-657.

Kathirvelu, K.P. and R. Balasubramanian, 2014. Design and implementation of PS-ZVS full bridge converter. J. Applied Sci., 14: 1588-1593.

Lee, W.J.B., C.E. Kim, G.W. Moon and S.K. Han, 2008. A new phase-shifted full-bridge converter with voltage-doubler-type rectifier for high-efficiency PDP sustaining power module. IEEE Trans. Ind. Electron., 55: 2450-2458.

Mishima, T. and M. Nakaoka, 2011. Practical evaluations of a ZVS-PWM DC-DC converter with secondary-side phase-shifting active rectifier. IEEE Trans. Power Electron., 26: 3896-3909.

Nayak, D.K. and S.R. Reddy, 2011. Performance of the push-pull LLC resonant and PWM ZVS full bridge topologies. J. Applied Sci., 11: 2744-2753.

Pahlevaninezhad, M., P. Das, J. Drobnik, P.K. Jain and A. Bakhshai, 2012. A novel ZVZCS full-bridge DC/DC converter used for electric vehicles. IEEE Trans. Power Electron., 27: 2752-2769.

Sabate, J.A., V. Vlatkovic, R.B. Ridley, F.C. Lee and B.H. Cho, 1990. Design considerations for high-voltage high-power full-bridge zero-voltage-switched PWM converter. Proceedings of the 5th Annual IEEE Applied Power Electronics Conference and Exposition, March 11-16, 1990, Los Angeles, CA., USA., pp: 275-284.

Sabate, J.A., V. Vlatkovic, R.B. Ridley and F.C. Lee, 1991. High-voltage, high-power, ZVS, full-bridge PWM converter employing an active snubber. Proceedings of the 6th Annual Applied Power Electronics Conference and Exposition, March 10-15, 1991, Dallas, TX., USA., pp: 158-163.

Wu, X., J. Zhang, X. Xie and Z. Qian, 2006. Analysis and optimal design considerations for an improved full bridge ZVS DC-DC converter with high efficiency. IEEE Trans. Power Electron., 21: 1225-1234.

Yadav, G.N.B. and N.L. Narasamma, 2014. An active soft switched phase-shifted full- bridge DC-DC converter: Analysis, modeling, design and implementation. IEEE Trans. Power Electron., 29: 4538-4550.